

# Effect of the poloidal rotation of the turbulence in reflectometry measurements

S. Hacquin, S. Heuraux<sup>+</sup>, F. Silva, G. Leclert<sup>++</sup> M. Manso and F. Serra

*Centro de Fusão Nuclear – Associação EURATOM / IST, Instituto Superior Técnico, Av. Rovisco Pais, 1049-001 Lisboa, Portugal*

<sup>+</sup>*Laboratoire de Physique des Milieux Ionisés et Applications, UMR 7040 CNRS, Université Henri Poincaré, Nancy 1, BP 239, 54506 Vandœuvre Cedex, France*

<sup>++</sup>*Laboratoire PIIM, UMR 6633 CNRS, Univ. de Provence, Faculté de St Jérôme, Case 321, 13397 Marseille Cedex 20 France*

## I. Introduction

Reflectometry can be a useful diagnostic to get some information on the plasma density fluctuations <sup>[1]</sup>, which is key issue for the next fusion devices. In this paper the role of the poloidal rotation of the turbulence in reflectometry measurements is investigated from 2D full-wave simulations. First, in the case of a rotating chain of magnetic islands we show that information on the island size and rotation velocity could be extracted. Then we study the effect of the poloidal rotation of micro-turbulence, highlighting the role of the poloidal  $k$ -spectrum and of the Doppler shift for oblique probing incidence.

## II. Simulation of fluctuation reflectometry experiments

Modelling of O-mode reflectometry experiment under the cold plasma approximation is done solving the following 2D full-wave equation <sup>[2]</sup>:

$$\left[ \frac{\partial^2}{\partial t^2} - c^2 \frac{\partial^2}{\partial r^2} - c^2 \frac{\partial^2}{\partial \theta^2} + \frac{e^2}{\epsilon_0^2 m_e} n_e(r, \theta, t) \right] E(r, \theta, t) = 0 \quad [1]$$

where  $r$  and  $\theta$  represent respectively the radial and the poloidal directions in a Cartesian plane (we neglect the poloidal curvature so that the directions  $r$  and  $\theta$  are perpendicular). To introduce a poloidal rotation of the turbulence at the velocity  $V_\theta$ , we define the density as

$$n_e(r, \theta, t) = \langle n_e(r, \theta) \rangle + \delta n_e(r, \theta - V_\theta t) \quad [2]$$

All the simulations presented here have been obtained for a linear unperturbed density profile  $\langle n_e(r, \theta) \rangle$ . A TE10 mode is excited in a fundamental wave-guide to emit the probing wave and an H-plane sectoral horn antenna is used to give its directivity <sup>[3]</sup>. The signal reflected by the plasma is collected in five different antennas (the emitted one plus four other ones equidistantly located in the poloidal plane) in order to assess the effect of the plasma poloidal rotation (see figure 1). To discriminate the amplitude  $A(t)$  and the phase  $\varphi(t)$  variations induced by the density fluctuations, we simulate an I/Q detection technique. The received signal in each one of the wave-guide can be written as:

$$S(t) = A(t) \cos(\omega t - \varphi(t)) \quad [3]$$

where  $\omega$  is the probing frequency ( $2\pi \cdot 40$  GHz in the simulations presented here). After multiplying [3] by  $2 \cdot \cos(\omega t)$  and  $2 \cdot \sin(\omega t)$  respectively and using a low-pass filtering, we obtain the signals  $I(t)$  and  $Q(t)$  that include the plasma information:

$$I(t) = A(t).\cos(\varphi(t)) \quad \text{and} \quad Q(t) = A(t).\sin(\varphi(t)) \quad [4]$$

The phase and the amplitude variations can be easily extracted combining  $I(t)$  and  $Q(t)$ :

$$A(t) = \sqrt{I(t)^2 + Q(t)^2} \quad \text{and} \quad \varphi(t) = \text{Arc tan}[Q(t)/I(t)] \quad [5]$$

As done with experimental data, we also carry out a spectral analysis of the complex signal given by:

$$C(t) = I(t) + iQ(t) = A(t)e^{i\varphi(t)} \quad [6]$$

### III. Effect of the poloidal rotation of magnetic islands

In this section, we investigate the effect of the poloidal rotation of a chain of magnetic islands modelled by [4]:  $\delta n_e(r, \theta, t) = a_f \cdot n_e(r_f) \cdot \exp[-(r - r_f)^2 / w_f^2] \cdot \sin[k_f(\theta - V_\theta t) + \varphi_f]$  [7]

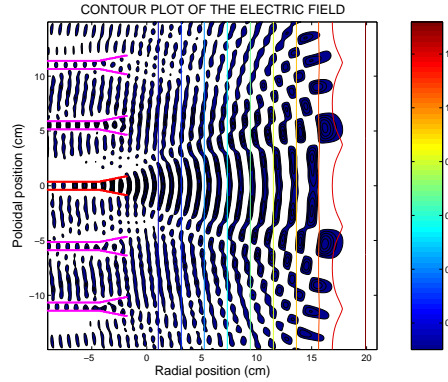


*Figure 1: Contour plot of the electric field during a simulation of poloidal propagation of a chain of magnetic islands (wave emission in the red wave-guide and reception in the 5 ones).*

We present a simulation obtained for the following parameters:  $a_f = 5\%$ ,  $r_f = r_c = 17.25$  cm,  $w_f = 1$  cm,  $k_f = 4\pi/30$  rad.cm $^{-1}$ ,  $\varphi_f = \pi/2$ . The number of time iterations has been chosen so that four magnetic islands pass in front of each antenna (i.e.  $V_\theta \cdot t_{obs} = V_\theta \cdot n \cdot \delta t = 4\pi/k_f = 30$  cm). A contour plot of the electric field (at the last time step) is represented in figure 1. The red wave-guide centred in the poloidal direction is used for emission of the probing wave as well as for reception of the reflected one. The magenta wave-guides symmetrically located around the red one are used for wave reception only. Let us note on the density contour plot the curvature of the cut-off layer induced by the magnetic islands. The amplitude and the phase of the reflected waves in each one of these wave-guides (given by [5]) are depicted in figure 2.

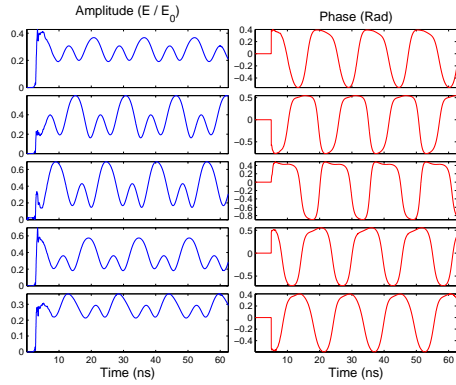


*Figure 2: Amplitude and phase of the reflected signals received in the 5 antennas (in decreasing values of poloidal position from the top to the bottom).*

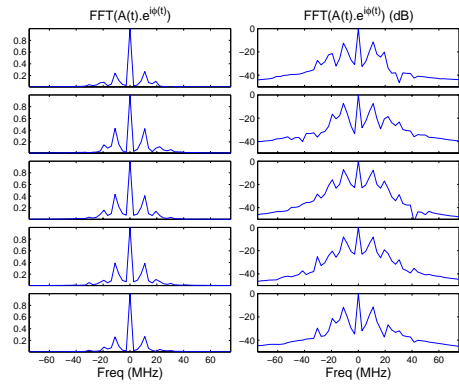


*Figure 3: Spectrum of the reflected complex signals received in the 5 antennas (linear scale on left and logarithmic scale on right).*

First of all we can notice that the amplitude of the reflected wave presents some primary and secondary maxima. The primary (or absolute) maxima appear when an X-point of a magnetic island passes in front of the antenna. In this case, the curvature of the cut-off layer

tends to reflect the maximum number of rays in the antenna. The secondary maxima occur when a 0-point of a magnetic island is located in front of the antenna. Ideally, the central (maximum amplitude) rays of the antenna radiation pattern are reflected in the antenna but the cut-off layer curvature tends to reflect the other rays away from the antenna. Moreover, phase maxima are seen for the X-points (furthest cut-off layer position) as phase minima correspond to the O-points (closest cut-off layer position). Assuming the cut-off is located at  $r = r_c$  for a X-point (minimum  $\delta n_e(r, \theta, t)$ ) and at  $r = r_c - r_c$  for a O-point (maximum  $\delta n_e(r, \theta, t)$ ), we can combine [2] and [7] to obtain:  $\Delta r_c = r_c \cdot a_f \cdot \exp[-\Delta r_c^2 / w_f^2]$  (valid only when the island is located at the cut-off layer). This gives  $\Delta r_c \approx 0.6$  cm for the parameters used here. Since the density profile is just deformed in the vicinity of the cut-off layer, the phase variation (between an X- and an O-points) gives:  $\Delta\phi = 4\pi f/c \int_{r_c - \Delta r_c}^{r_c} N(r) dr$ , that is, for a linear density profile:  $\Delta\phi = 8\pi f / 3c \cdot (\Delta r_c)^{3/2} / \sqrt{r_c}$ . For the chosen parameters, we obtain  $\Delta\phi \approx 1.25$  rad, which conforms to the variations shown in figure 2. Finally we can notice that the pattern of the amplitude and phase variations is shift by  $t_{shift}$  between 2 successive antennas. This can be explained by the fact that the absolute amplitude and phase maxima are obtained when an X-point is situated at the median between the emission and reception antennas. This allows evaluating the poloidal rotation velocity of the magnetic island chain since  $V_\theta = \Delta\theta_{ant} / 2t_{shift}$ . From figure 2, we can notice that  $t_{shift} \approx 5.5-6$  ns, which conform to the poloidal rotation velocity  $V_\theta$  input in this simulation. Figure 3 shows the corresponding spectrum of the reflected complex signals (given by [6]), illustrating as expected some peaks at  $f \approx \pm 15$  MHz (frequency of the  $A(t)$  and  $\phi(t)$  variations).

#### IV. Effect of the poloidal rotation of micro-turbulence

The turbulence is generated using a multi-modal model of density fluctuations [2]:

$$\delta n_e(r, \theta, t) = \sum_k \sum_{k_\theta} a(k_r, k_\theta) \cos(k_r r + k_\theta(\theta - V_\theta t) + \phi(k_r, k_\theta))$$

where  $a(k_r, k_\theta)$  fix their spectrum amplitude  $S(k_r, k_\theta)$  and the random choice of  $\phi(k_r, k_\theta)$  insures their non-coherent property. In the following, the rms value of density fluctuations (normalised to  $n_c$ ) is set to  $a_f = 2\%$ . We limit our study to the effect of the poloidal  $k_\theta$ -spectrum (then  $k_r$  is set to 0). To agree with experimental observations [5], the  $k_\theta$ -spectrum is defined by a plateau for  $k_\theta \leq k_{\theta lim}$  and decreases in  $k_\theta^{-3}$  for  $k_\theta \geq k_{\theta lim}$ .

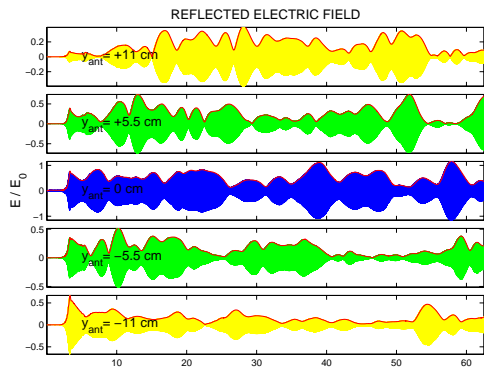


Figure 4: Reflected signals received in the 5 antennas (for fluctuations with  $k_{\theta lim} = 2 \text{ rad.cm}^{-1}$ ).

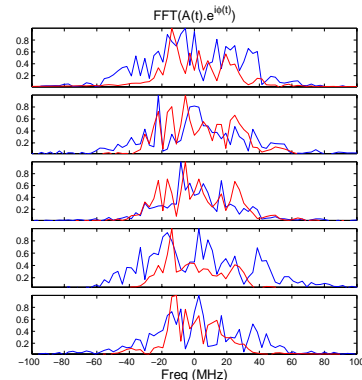


Figure 5: Signal spectrum; comparison between  $k_{\theta lim} = 0.5 \text{ rad.cm}^{-1}$  (red) and  $k_{\theta lim} = 2 \text{ rad.cm}^{-1}$  (blue).

First of all, figure 4 depicts the reflected signal received in the 5 antennas, showing how the turbulence can scatter the signal. The effect of the plateau limit  $k_{\theta lim}$  on the spectrum of the

reflected complex signal is shown in figure 5. For reception in the central antenna (also used for emission) no significant broadening is seen when  $k_{\theta\text{lim}}$  increases. A small broadening is noticeable for the decentred reception antennas, which is thought to be induced by Bragg scattering of some oblique rays of the antenna radiation pattern. However, this effect is not enough to observe a clear Doppler shift of the spectrum.

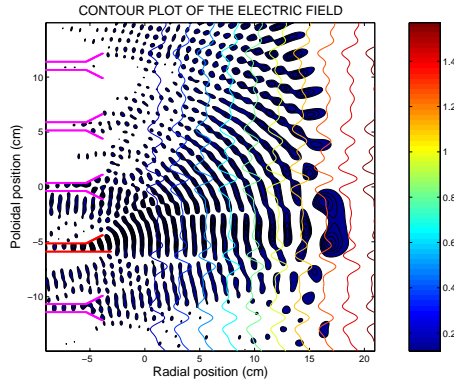


Figure 6: Contour plot of the electric field for an oblique incidence of the probing wave (use of an asymmetric emitting wave-guide).

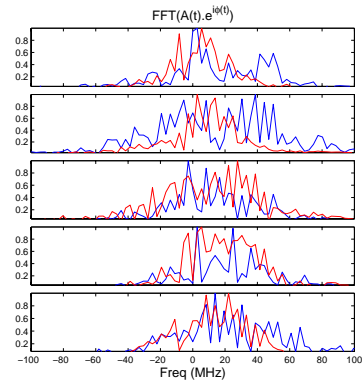


Figure 7: Spectrum of the reflected signals (for  $k_{\theta\text{lim}}=1 \text{ rad.cm}^{-1}$  in red and  $k_{\theta\text{lim}}=4 \text{ rad.cm}^{-1}$  in blue).

In order to see a significant Doppler effect, an asymmetry of the emitting antenna is introduced thus giving a probing oblique incidence (see figure 6). The frequency shift ( $\Delta\omega = k_\theta \cdot V_\theta$ <sup>[6]</sup>) induced by Doppler effect on the reflected signal spectra is illustrated in figure 7. This Doppler shift is especially strong for the 2 bottom reception antenna, which seems to indicate that the Bragg backscattering plays a major role in the Doppler shift. More simulations are required to confirm these preliminary results. In particular, the simulation time should be increased to improve the frequency resolution and the statistic information (which would require quite longer computing times).

## V. Conclusion

2D reflectometry simulations in the presence of poloidal rotation of density fluctuations are presented. It is shown that some information on either MHD activity or micro turbulence can be obtained from reflectometry signals. Additional studies are carried out to confirm these results in a more quantitative way. In particular, these simulations should allow a better understanding of the quantitative effect of the Doppler shift, which would help to interpret the Doppler reflectometry measurements.

## Acknowledgements

This work, supported by the European Communities and “Instituto Superior Técnico”, has been carried out within the Contract of Association between EURATOM and IST. Financial support was also received from “Fundação para a Ciência e Tecnologia” in the frame of the Contract of Associated Laboratory. The views and opinions expressed herein do not necessarily reflect those of the European Commission, IST and FCT.

## References:

- [1] E. Mazzucato, *Review of Scientific Instruments* **69**, 1691 (1998)
- [2] S. Heuraux *et al*, *Review of Scientific Instruments* **74** (3), 1501 (2003)
- [3] W. Stutzman and G. Thiele “Antenna Theory and Design”, Wiley, New York (1981)
- [4] F. Silva *et al*, *Review of Scientific Instruments* **74** (3), 1497 (2003)
- [5] P. Devynck *et al*, *Plasma Phys. Control. Fusion* **35**, 63 (1993)
- [6] X. L. Zou *et al*, 4<sup>th</sup> Int. Reflectometry workshop, CEA Cadarache, France (1999)